ELSEVIER

Catalysis Today 28 (1996) 167–174

CATALYSIS TODAY

# Layered niobium oxides — pillaring and exfoliation

K. Domen [a,*], Y. Ebina [a], S. Ikeda [a], A. Tanaka [b], J.N. Kondo [a], K. Maruya [a]

[a] *Research Laboratory of Resources Utilization, Tokyo Institute of Technology, 4259 Nagatsuta, Midori-ku, Yokohama 226, Japan*
[b] *Nikon Corporation, 1-10-1 Asamizodai, Sagamihara 228, Japan*

**Abstract**

Several ion-exchangeable layered niobates were applied to prepare modified layered photocatalysts. $K_{1-x}La_xCa_{2-x}Nb_3O_{10}$ ($x = 0$, 0.25, 0.50, 0.75), a layered perovskite series, with variable interlayer cation density, were used for the modification of the interlayer space by pillaring of silica and titania. The silica-pillaring process was monitored by NMR and the thermal stability was also examined. Silica-pillar was successfully introduced to all the series of perovskites which showed good photocatalytic activity. The preparation of titania-pillared layered niobates was more difficult. In the case of $KCa_2Nb_3O_{10}$ ($x = 0$), we could not introduce a titania pillar, but in the case of $K_{0.5}La_{0.5}Ca_{1.5}Nb_3O_{10}$ ($x = 0.5$) carrying less interlayer cation density, titania-pillar was introduced although the thermal stability was very poor. $K_4Nb_6O_{17}$, another type of layered niobate, was used for the exfoliation and restacking of the niobate sheets. The structure and photocatalytic activity of the product was examined.

*Keywords:* Niobium oxides; Layered niobates

## 1. Introduction

We have been studying the photocatalytic activity of various ion-exchangeable layered niobates. For further functionalization of these materials, modification by pillaring at the interlayer spaces or exfoliation of the niobate sheets has been recently carried out. Some results of the attempts, including preliminary ones, are reported.

Recently, several layered metal oxides have been demonstrated to be highly active photocatalysts under the band gap irradiation [1–8]. One of the characteristics of such a layered compound photocatalyst is to efficiently use intercalated molecules as reactants by a proper modification. Some niobate layered compounds, $A_4Nb_6O_{17}$ (A = K, Rb) for example, showed high quantum efficiency for an overall photodecomposition of water (10% on 0.1 wt.-% Ni–$Rb_4Nb_6O_{17}$ under irradiation at 330 nm) by loading of ultrafine Ni metal particles at the interlayer space [2,5,7,9]. Layered perovskite type niobates, $AB_{n-1}Nb_nO_{3n+1}$ (A = K, Rb or Cs; B = La, Ca, Pb and so on; $n = 2$ or 3) were also found to possess high activity for photocatalytic $H_2$ evolution from an aqueous methanol solution [3,8]. The family of layered perovskite type niobates has a wide variety of the composition; for example, when Pb was incorporated in the B site, photocatalytic hydrogen evolution under visible light irradiation ($\lambda > 420$ nm) proceeded [8]. Reactivity of the niobates was in-

* Corresponding author.


*SSDI* 0920-5861(95)00223-5

creased by substitution of $H^+$ ions for the alkali metal cations at the interlayer space which caused the intercalation of reactant molecules [10]. In general, however, reactant molecules including water are hardly intercalated into the interlayer space of the layered perovskite type niobate except the $H^+$-forms, which is probably due to the high charge density of the niobate layer. This makes the proper modification of interlayer space difficult for obtaining further functionalized photocatalysts.

In this study, two different methods were applied to modify the interlayer space, i.e., pillaring and exfoliation. The structural study of the products and their photocatalytic activities were carried out. The schematic structures of $K_{1-x}La_xCa_{2-x}Nb_3O_{10}$ and $K_4Nb_6O_{17}$ are depicted in Fig. 1.

## 2. Experimental

### 2.1. Layered materials

$K_{1-x}La_xCa_{2-x}Nb_3O_{10}$ was prepared according to the literature, reported by Uma and Gopalakrishnan [11]. A stoichiometric mixture of $K_2CO_3$, $La_2O_3$, $CaCO_3$ and $Nb_2O_5$ was calcined in a platinum crucible in air at 1473 K for 10 h. The XRD pattern was well coincided with that in literature [11–14]. In case of $K_4Nb_6O_{17}$, a stoichiometric mixture of $K_2CO_3$ and $Nb_2O_5$ were melted in a platinum crucible at 1473 K and then cooled down rapidly to form large crystals. These were pulverized in a mortar. $H^+$-exchanged form was prepared by an ion-exchange method. For instance, $HCa_2Nb_3O_{10}$ was prepared by ion-exchange of $KCa_2Nb_3O_{10}$ (20 g) in 5 mol $dm^{-3}$ $HNO_3$ (400 $cm^3$) solution for 72 h at room temperature (degree of $H^+$-exchange > 95%). Alkylamines (alkyl = octyl, dodecyl and octadecyl; in two equivalents) were intercalated into $HCa_2Nb_3O_{10}$ (20 g) by refluxing in heptane (100 $cm^3$) for 1–3 days (bath temperature: 403 K).

### 2.2. Pillaring

A similar method, previously reported by Landis et al., was employed for silica pillaring [15]. An alkylammonium-exchanged niobate (20 g) was stirred in tetraethylorthosilicate (TEOS, 100 $cm^3$) at 353 K for 72 h, followed by filtering. The precipitate was washed with ethanol and then dried. The TEOS treatment was repeated twice. The treated sample was finally calcined at 773–973 K for 4 h in air. In the case of titania-pillaring, titanium tetraisopropoxide ($Ti(O^iPr)_4$) was added into 2 mol $dm^{-3}$ HCl aq. and stirred for 1 h at room

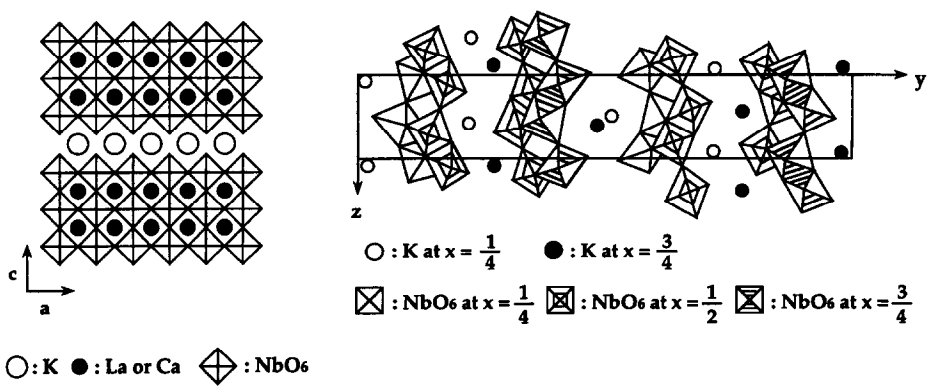


Fig. 1. Schematic structure of $K_{1-x}La_xCa_{2-x}Nb_3O_{10}$ and $K_4Nb_6O_{17}$.

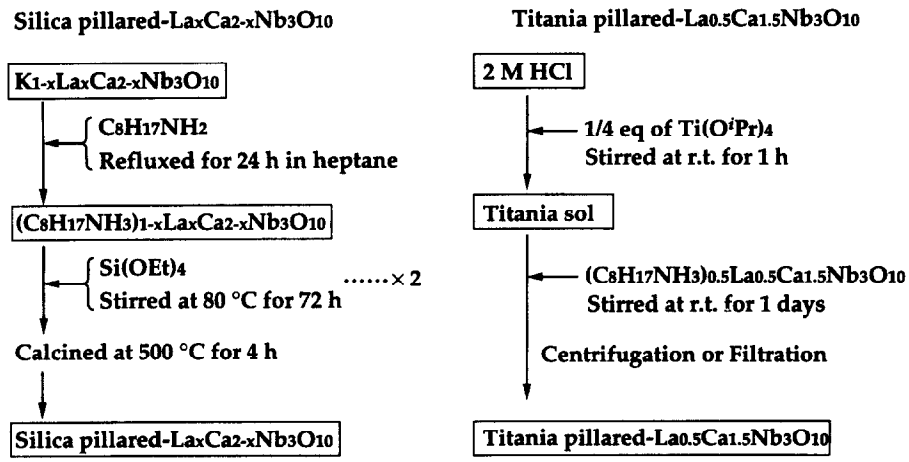


Scheme 1. Preparation of silica and titania pillared niobates.

temperature for peptization. After the solution became transparent, alkylammonium ion-intercalated niobate was immersed in the solution and was stirred for 1 day followed by centrifugation and drying. Schematic representation of the procedure is depicted in Scheme 1.

### 2.3. Exfoliation

$H_4Nb_6O_{17}$ was prepared by ion exchange from $K_4Nb_6O_{17}$ in a 0.25 mol $dm^{-3}$ $H_2SO_4$ solution. The $H_4Nb_6O_{17}$ was suspended in an aqueous tetrabutylammonium hydroxide ($TBA^+OH^-$) solution followed by centrifugation [16]. The top of the solution contained exfoliated niobate sheets which were homogeneously dispersed in the solution. These were precipitated by a dilute $HNO_3$ addition and were filtrated. The sediment was washed by 0.1 mol $dm^{-3}$ $HNO_3$ to remove $TBA^+$ and obtain a restacked $H_4Nb_6O_{17}$. The procedure is schematically shown in Scheme 2.

### 2.4. Characterization

For characterization of those products, X-ray powder diffraction (XRD, Rigaku Geigerflex RAD-B, Cu K$\alpha$), X-ray photoelectron spectroscopy (XPS, Shimazu ESCA 750), transmission electron microscopy (TEM, Hitachi HF-2000, 200 kV) and $^{29}Si$ CP/MAS NMR (JEOL GX-270) were used.

### 2.5. Photocatalytic reaction

Photocatalytic reaction was carried out in an air-free closed gas circulation system with an inner irradiation type reaction cell made of Pyrex (250 $cm^3$). The catalyst (1 g) was dispersed in an aqueous solution (330 $cm^3$) by magnetic stirring and was irradiated under Ar atmosphere

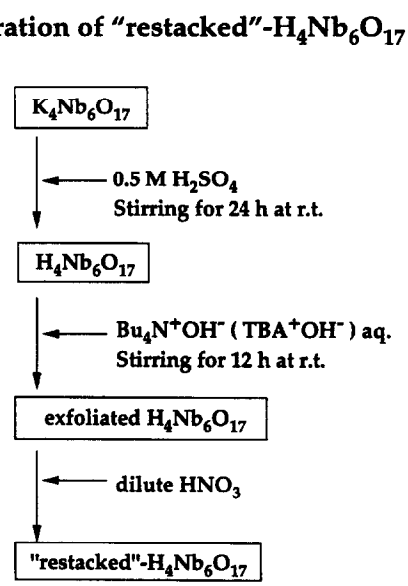


Scheme 2. Preparation of restacked $H_4Nb_6O_{17}$.

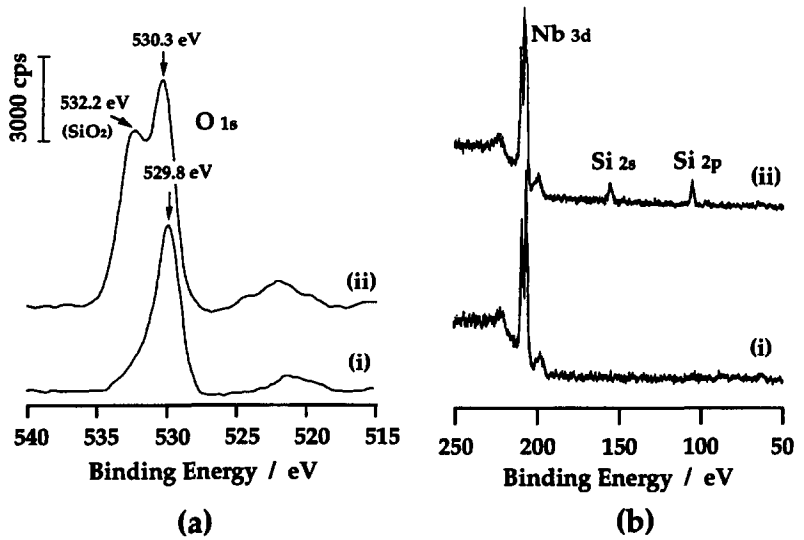


Fig. 2. XP spectra of (i) $HCa_2Nb_3O_{10}$, (ii) silica pillared-$Ca_2Nb_3O_{10}$. (a) O 1s, (b) Si 2s and 2p.

(about 13.3 kPa) by a high pressure Hg lamp (450 W). $H_2$ evolution was carried out in a 10 vol-% aqueous alcohol solution. Pt loading was carried out by a photodeposition method with addition of $H_2PtCl_6$ into the aqueous alcohol solution. The amount of evolved gas was analyzed by a gas chromatography (MS-5A column, Ar carrier) through a gas sampler (10 $cm^3$) which was directly connected to the reaction system to avoid any contamination from air.

## 3. Results and discussion

### *3.1. Characterization of silica pillared-$Ca_2Nb_3O_{10}$ by XPS and NMR*

Some structural studies including XRD on silica pillared-$Ca_2Nb_3O_{10}$ have been reported previously. Further spectroscopic studies by means of XPS and NMR are briefly mentioned. Comparison of XP spectra of $HCa_2Nb_3O_{10}$ and silica pillared-$Ca_2Nb_3O_{10}$ via octylamine intercalation is shown in Fig. 2. New peaks attributed to Si 2s and 2p, and an additional peak of O 1s at higher binding energy due to silica's oxygen were observed for the pillared sample. There was no obvious difference in peak intensities of other elements between the two spectra, indicating that little amount of silica covered the external surface; most of the silica existed in the interlayer. The ratio of Si and Nb at the surface was estimated from the peak intensities of XP spectra after normalization using relative sensitivity to give Nb: Si = 1: 0.71.

In Table 1 results of $^1H-^{29}Si$ CP/MAS NMR during TEOS treatment of $(C_8H_{17}NH_3)Ca_2Nb_3O_{10}$ are summarized. The sample which was once treated by TEOS possessed two peaks at −88.4 and −100.5 ppm, while a single peak at ca. −100 ppm appeared for the sample treated twice by TEOS and for that after calcination at 773 K. The peak at −88.4 ppm and those around −100 ppm are assigned to $Q^2$ and $Q^3$ (for the nomenclature

Table 1
Results of $^1H-^{29}Si$ CP/MAS NMR during TEOS treatment of $(C_8H_{17}NH_3)Ca_2Nb_3O_{10}$

| Samples | Chemical shift (ppm) | |
|---|---|---|
| Once treated by TEOS | −88.4 ($Q^2$) | −100.5 ($Q^3$) |
| Twice treated by TEOS | | −101.6 ($Q^3$) |
| Calcined of twice treated by TEOS (500°C) | | −98.6 ($Q^3$) |

Table 2
Type and chemical shift of solid silicates [a]

| Type of silicon–oxygen tetrahedra | $Q^0$ single | $Q^1$ end group | $Q^2$ middle group | $Q^3$ branching group | $Q^4$ cross-linking group |
|---|---|---|---|---|---|
| Structure | $Si(O^-)_4$ | $(SiO)Si(O^-)_3$ | $(SiO)_2Si(O^-)_2$ | $(SiO)_3Si(O^-)$ | $Si(SiO)_4$ |
| $^{29}Si$ chemical shift range from $Me_4Si$ | ca. −60 to −83 | ca. −67 to −85 | ca. −70 to −93 | ca. −90 to −102 | ca. −105 to −120 |

[a] Ref. [17].

$Q^n$, see the Table 2, [17]). It is noted that any peaks assigned to $Q^4$ were not observed for all samples, indicating very small amount of Si existed as a bulk $SiO_2$. Therefore, most of the Si is regarded as surface Si terminating with OH. It was also found that neither $Q^0$ nor $Q^1$ was observed for all samples. From this result, hydrolysis of TEOS in interlayer proceeds during the TEOS treatment. The appearance of $Q^2$ for the sample treated once by TEOS was probably due to the uncompleted hydrolysis. However, it was not observed after the second TEOS treatment. The shrinkage of the sample treated by TEOS once was probably due to the fact that not enough amount of TEOS has been intercalated. It is, therefore, concluded that the stable silica pillar mainly consists of $Q^3$ Si.

### 3.2. *Silica pillared-$La_xCa_{2-x}Nb_3O_{10}$*

In the above section, silica pillared-$Ca_2Nb_3O_{10}$ was successfully prepared and the unique photocatalytic activity was also demonstrated in the previous report. Then, we tried to prepare the pillared-$Ca_2Nb_3O_{10}$ using other materials such as titania and zirconia. However, all attempts were found to be unsuccessful. One of the reasons for the failure seems to be due to the high charge density of the niobate sheet which makes the stacking of the layers rigid. Therefore, we decided to use niobates which possess a less charge density in the niobate sheet. Uma and Gopalakrishnan reported a series of layered perovskite, $K_{1-x}La_xCa_{2-x}Nb_3O_{10}$, in which the charge density of the sheet is variable [11]. Before examining the pillared niobates, photocatalytic activity of the original niobates was studied. The results are shown in Table 3. The structures of all catalysts were confirmed by XRD. The $H^+$-exchanged forms were all hydrated and the interlayer spacings increased by ca. 0.2 nm. For all catalysts, $H_2$ evolution rate increased markedly by $H^+$-exchange suggesting the intercalation of methanol and water molecules. In the case of the lowest charge density catalyst, $x = 0.75$, the rate of $H_2$ evolution was much lower than those of others. This may be due to the difficulty of the intercalation of reactant molecules because of the lower charge density.

Silica pillared-$La_xCa_{2-x}Nb_3O_{10}$ ($x = 0.25$, 0.50 and 0.75) was prepared in the same way as that applied to the sample of $x = 0$, $HCa_2Nb_3O_{10}$. The c-axis lengths and BET surface areas are listed as well as the $H_2$ evolution rate from an aqueous methanol solution in Table 4. For the samples with $x = 0.25$ and $x = 0.5$ similar structures and photocatalytic activity were obtained to that with $x = 0$, but the sample with $x = 0.75$ showed shorter c-axis length and much smaller BET surface area than the others. The rate of $H_2$ evolution was also slower than the others. These results may be again attributed

Table 3
Photocatalytic activities of layered perovskite compounds with variable interlayer cation density: $K_{1-x}La_xCa_{2-x}Nb_3O_{10}$

| Catalysts | Rate of $H_2$ evolution ($\mu$mol $h^{-1}$) | | | |
|---|---|---|---|---|
| | Original | | $H^+$-exchanged | |
| | Alone | Pt-loaded | Alone | Pt-loaded |
| $KCa_2Nb_3O_{10}$ | 10 | 100 | 2200 | 8700 |
| $K_{0.75}La_{0.25}Ca_{1.75}Nb_3O_{10}$ | 7.8 | 193 | 3490 | 11700 |
| $K_{0.50}La_{0.50}Ca_{1.50}Nb_3O_{10}$ | 6.1 | 215 | 2030 | 13500 |
| $K_{0.25}La_{0.75}Ca_{1.25}Nb_3O_{10}$ | 2.0 | 126 | 155 | 6530 |

Table 4
C-axis length, surface area and phtocatalytic activity for decomposition of water of layered perovskite compounds with variable interlayer cation density: $K_{1-x}La_xCa_{2-x}Nb_3O_{10}$

| Precursor | c-Axis length (nm) | | BET surface area ($m^2\ g^{-1}$) | Rate of $H_2$ evolution of silica pillared niobates ($\mu mol\ h^{-1}$) |
|---|---|---|---|---|
| | Before calcination | After calcination | | |
| $(C_8H_{17}NH_3)Ca_2Nb_3O_{10}$ | 3.26 | 2.93 | 200 | 10800 |
| $(C_8H_{17}NH_3)_{0.75}La_{0.25}Ca_{1.75}Nb_3O_{10}$ | 3.31 | 2.95 | 320 | 11200 |
| $(C_8H_{17}NH_3)_{0.50}La_{0.50}Ca_{1.50}Nb_3O_{10}$ | 3.29 | 2.95 | 110 | 14700 |
| $(C_8H_{17}NH_3)_{0.25}La_{0.75}Ca_{1.25}Nb_3O_{10}$ | 3.33 | 2.76 | 48 | 7900 |

to the lower charge density of the sample with $x = 0.75$.

### 3.3. Titania pillared-$La_{0.5}Ca_{1.5}Nb_3O_{10}$

As mentioned above, we tried to prepare the titania-pillared niobate photocatalysts from $HCa_2Nb_3O_{10}$, but the attempt did not succeed due to the high charge density of the niobate layer which prevented the expansion of the interlayer space and the intercalation of the precursor materials of the titania pillar. Therefore, layer-charge density controlled perovskite-type niobates, i.e., $K_{1-x}La_xCa_{2-x}Nb_3O_{10}$ $(0 \le x < 1)$, were prepared. By using the sample with $x = 0.5$ titania-pillared layered photocatalyst was prepared. The detailed procedure was mentioned in the experimental section. The XRD pattern of each step is shown in Fig. 3. The final step of the procedure is the ion-exchange alkylammonium cations in the layered niobate and positively charged titania sol. The sample was dried at room temperature. By this treatment, alkylammonium cations were almost completely removed because no indicative peak of alkylammonium burning was observed in TG measure-

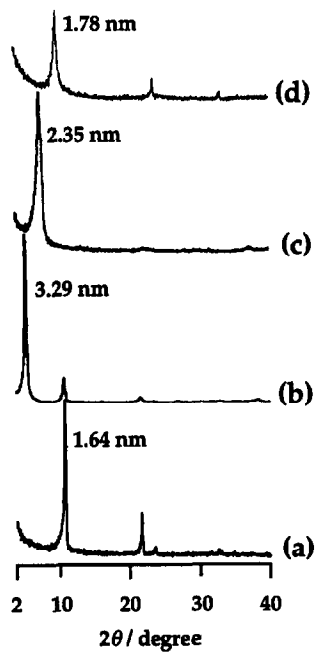


Fig. 3. XRD pattern of (a) $H_{0.5}La_{0.5}Ca_{1.5}Nb_3O_{10}$, (b) $(C_8H_{17}NH_3)_{0.5}La_{0.5}Ca_{1.5}Nb_3O_{10}$, (c) titania pillared-$La_{0.5}Ca_{1.5}Nb_3O_{10}$ (dried at rt in air) and (d) titania pillared-$La_{0.5}Ca_{1.5}Nb_3O_{10}$ (calcined at 200°C for 24 h).

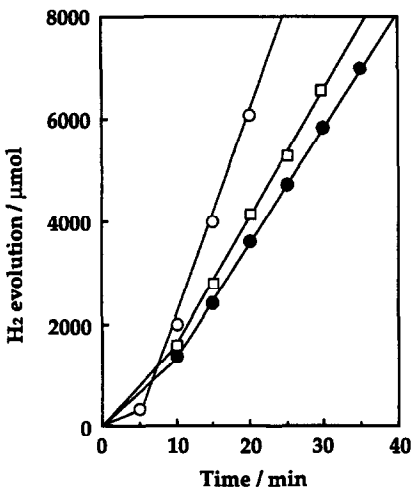


Fig. 4. $H_2$-evolution with several layered niobates. ●: $H_{0.5}La_{0.5}Ca_{1.5}Nb_3O_{10}$, □: silica pillared-$Ca_{1.5}Nb_3O_{10}$, ○: titania pillared-$Ca_{1.5}Nb_3O_{10}$.

ment. The interlayer space was expanded for about 0.7 nm from the original $H^+$-exchanged form. This expansion is attributed to the intercalation of small positively charged titania sol. The titania-pillared catalyst was, however, thermally unstable, e.g., the calcination of the sample at 573 K caused the shrinkage of the interlayer spacing, i.e., 1.8 nm of the c-axis length. The photocatalytic activity of $H_2$ evolution from an aqueous methanol solution was higher than that of silica-pillared or $H^+$-exchanged photocatalyst as shown in Fig. 4. The high photocatalytic activity of the titania-pillared photocatalyst suggests a promising application but the thermal stability must be improved.

### 3.4. Exfoliated $H_4Nb_6O_{17}$

Some XRD patterns of these samples are shown in Fig. 5. Fig. 5a is of $H_4Nb_6O_{17}$ which gives a strong (040) diffraction peak indicating well ordered stacking of niobate sheets. Shown in Fig. 5b is the XRD pattern of the top solution being centrifuged, evaporated and dried. Although three broad peaks, suggesting a layered structure, are observed, the intensities are very weak compared to those of Fig. 5a. These three peaks may be indexed as shown in Fig. 5b and the estimated b-axis length is about 4.6 nm which is too short to assign to the $TBA^+$-intercalated structure. Therefore we tentatively attribute these peaks to $H_4Nb_6O_{17} \cdot xH_2O$ ($x >$ 4.5), because $K_4Nb_6O_{17} \cdot 4.5H_2O$ is produced when $K_4Nb_6O_{17}$ is immersed in an aqueous solution and it gives a b-axis length of 4.1 nm. The results of TG measurements of the sample

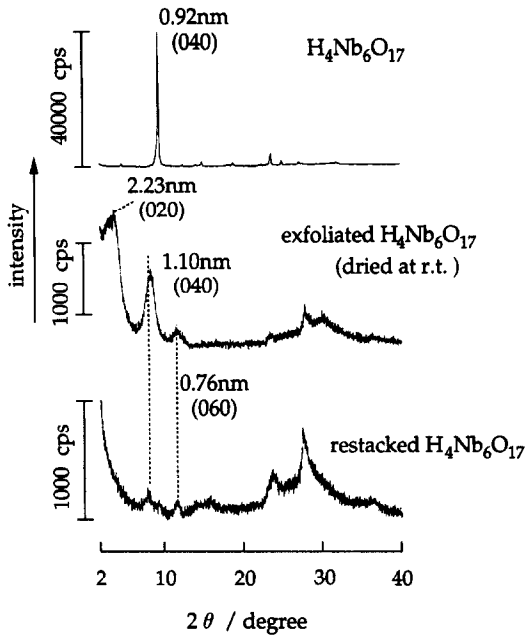


Fig. 5. XRD pattern of (a) $H_4Nb_6O_{17}$, (b) dried sample of exfoliated $HK_4Nb_6O_{17}$ and (c) restacked $H_4Nb_6O_{17}$.

in Fig. 5b suggested $x$ was 8–10. From these considerations, the weak peaks observed in Fig. 5b come from a small amount of remaining $H_4Nb_6O_{17}$ in which intercalation of $TBA^+$ does not occur to exfoliate the niobate sheets. Most part of the niobate sheets are exfoliated in the solution and these does not give an XRD pattern. When the exfoliated sheets were precipitated by an aqueous $HNO_3$ solution (Fig. 5c), the XRD peaks became much weaker and the relative peak intensity relevant to the b-axis length were weaker than those to the in-plane direction. This indicates that the stacking of the niobate sheets are very poor but the two dimensional sheet structure may remain. Such a struc-

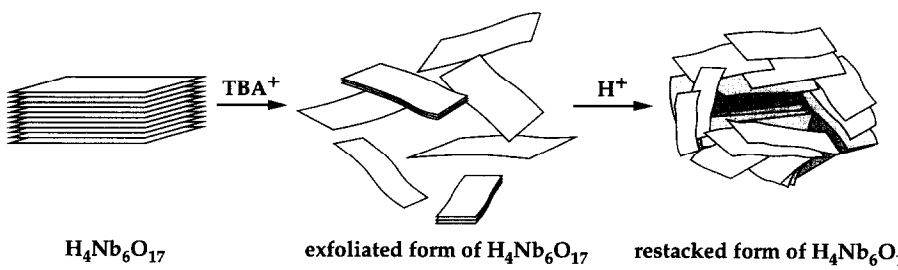


Scheme 3. The transformation process of exfoliation and restacking.

Table 5
Rate of $H_2$ evolution from aqueous alcohol solution ($\mu$mol $h^{-1}$)

| Catalyst | Methanol | | Ethanol | | n-Propanol | |
|---|---|---|---|---|---|---|
| | Alone | Pt, 1 wt.-% loaded | Alone | Pt, 1 wt.-% loaded | Alone | Pt, 1 wt.-% loaded |
| $H_4Nb_6O_{17}$ | 2720 | 3800 | 225 | 110 | 110 | 40 |
| Restacked $H_4Nb_6O_{17}$ | 490 | 3200 | 405 | 1350 | 270 | 720 |
| $Nb_2O_5 \cdot xH_2O$ | 220 | 900 | 270 | 660 | 85 | 430 |

ture was also supported by the SEM photographs, on which rather loosely and irregularly piled-up niobate sheets were observed. The basic idea of this transformation process is depicted in Scheme 3. It is noticed that the BET surface area of the sample in Fig. 5c is 108 $m^2$ $g^{-1}$ after evacuation at 473 K while it was only 4 $m^2$ $g^{-1}$ for the sample in Fig. 5a.

Photocatalytic activities of $H_2$ evolution from several aqueous alcohol solutions were compared with $H_4Nb_6O_{17}$ (Fig. 5a), restacked $H_4Nb_6O_{17}$ (Fig. 5c) and amorphous $Nb_2O_5 \cdot xH_2O$ prepared from an aqueous $K_8Nb_6O_{19}$ solution by acid hydrolysis (Table 5) [18,19]. For $H_4Nb_6O_{17}$, methanol was the most suitable reducing reagent and the rate of $H_2$ evolution decreased markedly in ethanol and n-propanol solutions. This result was interpreted by the structure selectivity of the layered niobate in which alcohols are oxidized in the interlayer space. On the other hand, restacked $H_4Nb_6O_{17}$ showed much less structure selectivity compared to the $H_4Nb_6O_{17}$. Especially, in ethanol and n-propanol solutions restacked $H_4Nb_6O_{17}$ with Pt-deposition exhibited much higher activity for $H_2$ evolution. This may be the result of the poor ordering of the niobate sheets and the interlayer spacing being broader in average. Restacked $H_4Nb_6O_{17}$ showed a more similar tendency of $H_2$ evolution reaction to amorphous $Nb_2O_5 \cdot xH_2O$ than $H_4Nb_6O_{17}$, which is reasonably understood by the structural consideration.

## References

[1] K. Domen, A. Kudo, A. Shinozaki, A. Tanaka, K. Maruya and T. Onishi, J. Chem. Soc., Chem. Commun., (1986) 356.
[2] K. Domen, A. Kudo, M. Shibata, A. Tanaka, K. Maruya and T. Onishi, J. Chem. Soc., Chem. Commun., (1986) 1706.
[3] K. Domen, J. Yoshimura, T. Sekine, A. Tanaka and T. Onishi, Catal. Lett., 4 (1990) 339.
[4] A. Kudo, M. Steinberg, A. J. Bard, A. Campion, M. A. Fox, T. E. Mallouk, S. E. Webber and J. M. White, Catal. Lett., 5 (1990) 61.
[5] A. Kudo, K. Sayama, A. Tanaka, K. Asakura, K. Domen, K. Maruya and T. Onishi, J. Catal., 120 (1989) 337.
[6] K. Sayama, A. Tanaka, K. Domen, K. Maruya and T. Onishi, Catal. Lett., 4 (1990) 217.
[7] K. Sayama, A. Tanaka, K. Domen, K. Maruya and T. Onishi, J. Phys. Chem., 95 (1991) 1345.
[8] J. Yoshimura, Y. Ebina, J. Kondo, K. Domen and A. Tanaka, J. Phys. Chem., 97 (1993) 1970.
[9] A. Kudo, A. Tanaka, K. Domen, K. Maruya, K. Aika and T. Onishi, J. Catal., 111 (1988) 67.
[10] A. J. Jacobson, J. W. Jacobson and J. T. Lewandowski, Mater. Res. Bull., 22 (1987) 45.
[11] S. Uma and J. Gopalakrishnan, J. Solid State Chem., 102 (1993) 332.
[12] M. Dion, M. Ganne and M. Tournoux, Rev. Chim. Min., 23 (1986) 61.
[13] M. Dion, M. Ganne and M. Tournoux, Mater. Res. Bull., 16 (1981) 1429.
[14] A. J. Jacobson, J. T. Lewandowski and J. W. Johnson, J. Less-Common Metals, 116 (1986) 137.
[15] M. E. Landis, B. A. Aufdembrink, P. Chu, I. D. Johnson, G. W. Kirker and M. K. Rubin, J. Am. Chem. Soc., 113 (1991) 3189.
[16] S. W. Keller, H.-N. Kim and T. E. Mallouk, J. Am. Chem. Soc., 116 (1994) 8817.
[17] E. Lippmaa, M. Mägi, A. Samonson, M. Tarmak and G. Engelhardt, J. Am. Chem. Soc., 103 (1981) 4992.
[18] B. K. Sen and A. V. Saha, Mater. Res. Bull., 17 (1982) 1982.
[19] B. K. Sen, A. V. Saha and N. Chatterjee, Mater. Res. Bull., 16 (1981) 923.